Chinese Chemical Letters 37 (2026) 111931

Contents lists available at ScienceDirect

Chinese Chemical Letters

journal homepage: www.elsevier.com/locate/cclet

A universal strategy based carbonized polymer dots self-assembled supramolecular oleogel lubricants *via* chain entanglement for friction reduction and anti-wear

Pai Yu[a,b], Chenchen Wang[b,*], Hualin Lin[b,*], Sheng Han[a,b,*]

[a] School of Chemistry and Chemical Engineering, Shihezi University, Shihezi 832003, China
[b] Chemical and Environmental Engineering, Shanghai Institute of Technology, Shanghai 201418, China

ARTICLE INFO

Article history:
Received 24 February 2025
Revised 25 August 2025
Accepted 29 September 2025
Available online 30 September 2025

Keywords:
Anti-friction and anti-wear
Supramolecular gel
Carbonized polymer dots
Chain entanglement
Lubricant film

ABSTRACT

Developing a supramolecular polymer gel based on carbonized polymer dots with highly efficient lubrication properties is very challenging. Here, we obtained a kind of carbonized polymer dots (CPDs) by thermal reflux of long-chain aliphatic amines in halogenated benzene solvents. The CPDs nano-gel achieved high lubrication performance due to entangling effect of long chain and reversible thixotropic behavior after gel formation. Two-dimensional correlation synchronous (2D-COS) showed the CPDs connect small carbon dots into large hydrophobic structures through their own dense chain entanglement, thus trapping oil to form gel. Chain entanglement, as a non-permanent crosslinking, can slide under stress, and this flexible and dynamic characteristic allows it to maintain efficient and long-lasting lubrication without hysteresis during friction. The tribological test results showed a significant reduction of 38.14% in the coefficient of friction and 93.71% in wear scar diameter after lubrication with CPDs nano-gel. Moreover, the serial analysis for the friction interface and computational methodologies revealed that the formation of tribochemical film between friction pairs is the key to reduce wear. This study underscored the possibility of utilizing carbonized polymer dots for self-assembly applications, and we anticipate that supramolecular carbonized polymer dots gels have great potential in lubrication and emission reduction, ultimately contributing to the development of a sustainable society.

© 2026 Published by Elsevier B.V. on behalf of Chinese Chemical Society and Institute of Materia Medica, Chinese Academy of Medical Sciences.

With the rapid development of modern industry, higher requirements have been put forward for the performance of mechanical equipment. The working environment for the rotating components of transmission devices is becoming increasingly harsh, leading to lubrication failure, and even peeling and fracture in the contact areas of these rotating components, which seriously impacts their service life [1,2]. Friction not only results in energy waste and economic losses, but can also trigger production accidents. According to reports, over 30% of energy consumption is used to overcome friction; about 80% of machine components fail due to wear and tear; >50% of mechanical equipment accidents are caused by lubrication failure or excessive wear [3]. Reducing the energy loss caused by friction was used to extend the service life of mechanical systems, usually through efficient lubrication materials [4]. Among them, the application of liquid lubrication was more extensive and diverse [5]. However, the characteristic of liquid lubricants is that they are prone to leakage and volatilization, resulting in reduced lubrication effect, and may even cause pollution to the equipment or the use environment [6]. Lubricating grease could avoid the above problems, but it faces complex processes, and long operation time [7]. Therefore, it is essential to develop a simple and effective method for constraining liquid lubricants to avoid oil leakage and excessive viscous resistance.

Recently, supramolecular gel has been used as lubricant in the field of friction [8]. Supramolecular gels are usually formed by small molecules in selected solvent media through a variety of non-covalent interactions, including hydrogen bonding, van der Waals forces, π-π stacking, London dispersion force, dipole-dipole, hydrophobic interactions, and electrostatic interactions [9], which can spontaneously aggregate in solvent to form three-dimensional network structure [10]. This network structure contains many cavities that can accommodate a large number of organic and water molecules, forming a jelly like semi-solid structure of the system [11]. Those gels with the characteristics of flexible adjustment driv-

* Corresponding authors.
E-mail addresses: wangchenchen76@163.com (C. Wang), lhl6534@163.com (H. Lin), hansheng654321@sina.com (S. Han).

https://doi.org/10.1016/j.cclet.2025.111931
1001-8417/© 2026 Published by Elsevier B.V. on behalf of Chinese Chemical Society and Institute of Materia Medica, Chinese Academy of Medical Sciences.

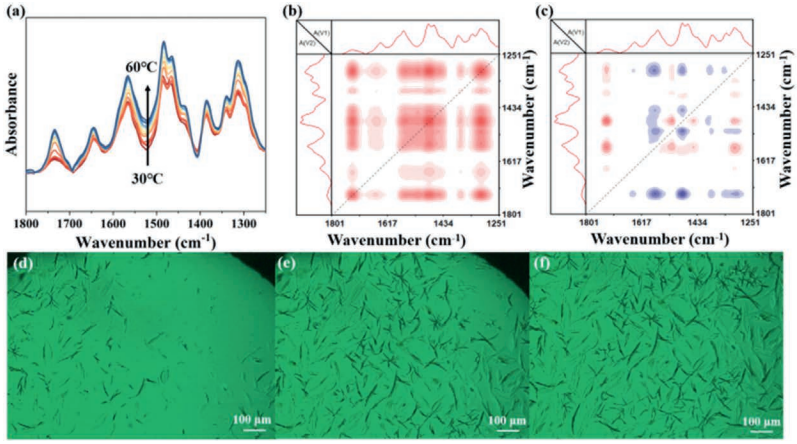


Fig. 1. (a) Temperature-dependent Fourier transform infrared (FT-IR) spectra of CPDs nano-gel, synchronous (b) and asynchronous (c) spectra of the CPDs nano-gel. The opposite variation directions of the band intensity are represented by the pink and blue colors, respectively. POM of 12.5 wt% CPDs nano-gel at 50 °C (d), 40 °C (e) and 30 °C (f).

ing forces generally benefit from dynamic noncovalent interactions, which are usually lacking in the chemically cross-linked polymeric gels. So far, most organic gels belong to small molecular organic gels. These small molecules are interconnected by non-covalent bonds and exhibit polymer properties in solution. Under external stimulation, they can be reversibly transformed between aggregates and monomers. However, sometimes the mechanical properties and viscoelasticity of gels composed of small molecules can not meet the requirements. At present, there have been studies using polymer-based gels to solve the above problems [12,13], but these studies are still based on linear polymer hydrogels, which are relatively rare in the fixation of organic solvents or oils. Therefore, it is necessary to develop a kind of polymer organic gel factor which can form stable crosslinking.

Inspired by our previous work [14] on carbon dot aggregates as lubricant additives, this myristylamine-derived carbonized polymer dots (CPDs) fabricated *via* thermal reflux demonstrate autonomous gelation behavior. Two-dimensional correlation synchronous spectrum (2D-COS) and polarizing optical microscope (POM) were used to investigated the gel process of CPDs *in situ*. The results showed that because there were abundant hydrophobic chains on the surface of CPDs dissolved in polyalphaolefin (PAO), the chains would cross and tangle, and eventually form aggregates. These aggregates will become gel when they absorb solvents. Unlike chemical crosslinking, chain entanglement can slide against each other under stress. The tribological test results showed a significant reduction of 38.14 % in the coefficient of friction (COF) and 93.71 % in wear scar diameter (WSD) after lubrication with CPDs nano-gel. Through chemical analysis of the friction surface and computational modeling of the lubrication state, explored the potential friction mechanisms was the formation of tribochemical film between friction pairs is the key to reduce wear. This highly effective gel lubricant is simply prepared by CPDs, which provides a promising energy saving method. It is critical to improve the service life and reliability of transmission rotating parts, and is conducive to the sustainable development of the environment and ecosystem.

The synthesis steps of the CPDs are shown in Fig. S1 (Supporting information), spectral and structural information are given in Figs. S2 and S3 (Supporting information). The thermal properties and rheological properties of the CPDs nano-gel are given in Figs. S4 and S6 (Supporting information), which showed that CPDs nano-gel formed gel due to some interactions, and the sol/gel transition occurred with the increase and decrease of temperature. In order to obtain the changes in the temperature response mechanism of CPDs nano-gel, the coagulation/sol process of CPDs nano-gel was investigated *in situ*.

The temperature response mechanism of CPDs nano-gel can be revealed by the temperature dependent FT-IR (Fig. S6). Fig. S6 showed temperature dependent band mainly occurs between 1250 cm^{-1} and 1800 cm^{-1}, as shown in Fig. 1a, when magnified, as the temperature increased, the changes in the 1734, 1644, 1566 cm^{-1} band became increasingly apparent, belonging to the stretching vibration of double bonds (C=O). The same situation also occurred in the 1484, 1385, and 1313 cm^{-1} bands, which belong to the C–H. During the heating process, the molecular structure or chain conformation of temperature responsive polymers will change, while infrared spectroscopy can analyze the changes in molecular structure or chain conformation by capturing the frequency changes of molecular groups [15]. Fig. 1a showed that this change with temperature was caused by hydrogen bonding or changes in molecular conformation. However, due to the serious overlap of signals detected by conventional infrared or Raman spectroscopy tests, weak signals are masked, making it difficult to analyze the information changes during dynamic changes.

In order to obtain the fine structure and temperature response mechanism changes of temperature responsive polymers, the kinetic sequence of the thermal response of C=O and C–H could be further analyzed by 2D-COS (Figs. 1b and c), which was applied with the synchronous spectra and asynchronous spectra. There are four cross peaks (1734, 1734), (1566, 1566), (1485, 1485), and (1313, 1313) in the synchronous spectrogram, and three main automatic peaks (1734, 1485), (1734, 1566), and (1566, 1313) in the asynchronous spectrogram. Among them, 1734 and 1566 cm^{-1} correspond to C=O bending vibration, while 1485 and 1313 cm^{-1} correspond to C–H bending vibration, which all peaks corresponded and no sub peaks. Therefore, changes caused by hydrogen bonds can be excluded [16]. According to the Nado rule [17], the order of absorption peak response during the heating process is 1734 → 1556 → 1313 → 1485, indicating that during the heating process, C=O has a better response to temperature than C–H. Therefore, there is a conformational change but no chemical bond change in CPDs.

To further verify the conformational change, POM was used to track the real-time state of the CPDs nano-gel during the cooling process, and observed the growth and gel of CPDs polymer *in situ*, as shown in Figs. 1d-f and Figs. S5d-f (Supporting information). With the decrease of temperature, the CPDs was reassembled into some nanofibers with a diameter of over 100 nm, which conforms to the theory of crystal mismatch [18], when the undercooling is low, the nucleation potential barrier of crystal mismatch is very high, so the fibers tend to grow in one dimension, and the degree of fiber branching and entanglement is relatively

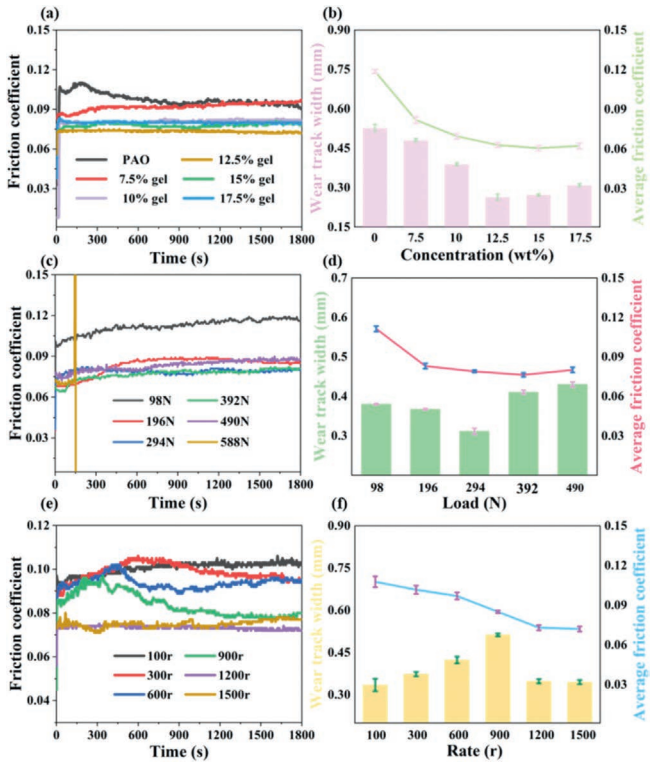


Fig. 2. (a) Coefficient of friction curves of CPDs nano-gel with different concentrations under 294 N, 1200 rpm, 25 °C. (b) CPDs nano-gel average coefficient of friction and wear volume under different concentrations under 294 N, 1200 rpm. (c) Coefficient of friction curves of 12.5 wt% CPDs nano-gel with different load (1200 rpm, 25 °C) and (d) 12.5 wt% CPDs nano-gel average coefficient of friction and wear volume under different load (1200 rpm, 25 °C). (e) Coefficient of friction curves of 12.5 wt% CPDs nano-gel with different rate (294 N, 25 °C) and (f) 12.5 wt% CPDs nano-gel average coefficient of friction and wear volume under different rate (294 N, 25 °C).

low. On the contrary, it will cause branching at the tips of the fiber.

Investigations were conducted systematically to assess lubricating property, polymer gels with concentrations of 7.5 wt%, 10.0 wt%, 12.5 wt%, 15 wt% and 17.5 wt% were tested by four-ball method (Fig. 2). As shown in Figs. 2a and b, under friction test at 294 N, compared with CPDs nano-gel, the friction coefficient for PAO experienced obvious fluctuations and increased first and then decreased, accompanied by the maximum wear trajectory width. Compared with the PAO, the COF and the WSD for the CPDs nano-gel decreased obviously. Meanwhile, with the increase of CPDs content, the COF and WSD of CPDs nano-gel would decrease then level off. It can be reasonably inferred that CPDs not only captures PAO to form the gel, but also exists in the base oil in the form of a lubricant additive. Meanwhile, to be as reliable oil-lubrication materials, it is necessary to investigate its lubrication behavior under high loads. So, the anti-wear property of the CPDs nano-gel was investigated upon applying different load (Fig. 2c). The minimum wear was obtained at 294 N (Fig. 2d). For CPDs nano-gel, lubrication failure occurred at 588 N, far greater than pure PAO (480 N, Fig. S7 in Supporting information), explained CPDs nano-gel has better carrying capacity. The influence of rotational speed on the friction coefficient of CPDs nano-gel showed that the friction coefficient was larger at low rotational speed, but decreases at high rotational speed. And the wear area increased initially and then decreased with the increasing rotational speed (Fig. 2f). At low speed (Fig. 2e), friction mainly came from indentation caused by steel surface wear. At this time, the temperature of the contact surface was low, and it was not easy to form an oxide film, so the friction coefficient was relatively large. With the increase of rotational speed, the contact surface generated a lot of heat, which helped the formation of oxide film. The presence of an oxide film helped to reduce direct contact, thereby reducing the coefficient of friction.

Further observations were conducted to assess wear conditions, focusing on the three-dimensional morphology, corresponding section curve, and SEM images of the wear surface (Fig. 3). As shown in Fig. $3a_1$-a_4, the wear surface after PAO lubrication was a large deep pit with a wear volume of $2.94 \times 10^5\ \mu m^3$. It was accompanied by rough wear marks, including deep furrows, micropits, and high bulges, which indicated that the contact points had severe adhesive wear under PAO. By contrast, the CPDs nano-gel effectively prevents further wear and tear. As can be seen from Fig. $3d_1$-d_4, the wear volume after 12.5 wt% CPDs nano-gel lubrication was significantly reduced ($1.85 \times 10^4\ \mu m^3$), which was only 6% of the wear volume after PAO lubrication. At the same time, it was observed that the wear track was smooth, which greatly alleviates the adhesive wear of steel contact. The wear volumes of 7.5 wt% (Fig. $3b_1$-b_3), 10 wt% (Fig. $3c_1$-c_3), 15 wt% (Fig. $3e_1$-e_3) and 17.5 wt% (Fig. $3f_1$-f_3) CPDs nano-gel were reduced to 2.07×10^5, 8.85×10^4, 2.11×10^4 and $3.52 \times 10^5\ \mu m^3$, respectively. It follows that CPDs nano-gel could significantly improve its anti-wear properties. To test the above hypothesis, X-ray photoelectron spectroscopy (XPS) was used for examining the surface information of the worn surface.

The lubricant at the contact point may react chemically with the friction pair during the friction process. In order to analyze the interface interaction between the CPDs nano-gel and the steel ball, the wear surface after the PAO and 12.5 wt% CPDs nano-gel were compared by XPS spectra. As shown in Figs. 4a, c, e and g, under the lubrication of PAO and CPDs nano-gel, C–O and O–C-O bonds (C 1s: 286.6 and 288.7 eV; O 1s: 531.6 and 533.1 eV) existed on the friction pair surface [19,20]. This indicated that an organic layer containing carbonyl and hydroxyl compounds had formed on the surface of the steel [21]. At the same time, the C–O-C peak intensity was high under the lubrication of CPDs nano-gel, which most likely originates from the frictional degradation of PAO and CPDs in the gel system, while under the lubrication of PAO, layer produced comes from frictional degradation of PAO. N 1s (Fig. 4f) shows that compared with before friction (Fig. S3e in Supporting information), two new peaks were detected on the worn surface, belonging to the Fe-N coordination bond (399.48 eV) and the oxidized nitrogen (401.68 eV) [22], proving that N is involved in the coordination and oxidation processes. Meanwhile, compared with PAO as a lubricant (Fig. 4b), Fig. 4f shows a new peak (-NH_4^+) confirms a more complex and effective tribochemical reaction under the lubrication of CPDs nano-gel, yielding a superior lubricating film.

The results shown in Figs. 4d and h supported the above conjecture, Fe 2p spectra showed exists Fe $2p_{3/2}$ and Fe $2p_{1/2}$ of Fe^0, which were at 707.0 and 719.6 eV, Fe $2p_{3/2}$ and Fe $2p_{1/2}$ of Fe_2O_3, which were at 710.5 and 723.9 eV [23]. Combined with O 1s (529.8 eV), indicating the presence of Fe_2O_3 in the formed tribolayer, which was caused by frictional chemical reaction between steel and dissolved water and oxygen in lubricants. The Fe_2O_3 had been proven to have an excellent friction-reducing effect [24], but had weaker wear resistance and lower shear strength. Therefore, when only PAO was used as lubricant, Fe and Fe_2O_3 were detected on the wear trajectory because Fe_2O_3 is continuous abrasion and regeneration (Fig. 4d). In comparison, the CPDs nano-gel lubricated surface showed that only Fe_2O_3 exists, indicating that the Fe_2O_3 was protected effectively by adsorbed CPDs and the steel ball had not been further worn down (Fig. 4h).

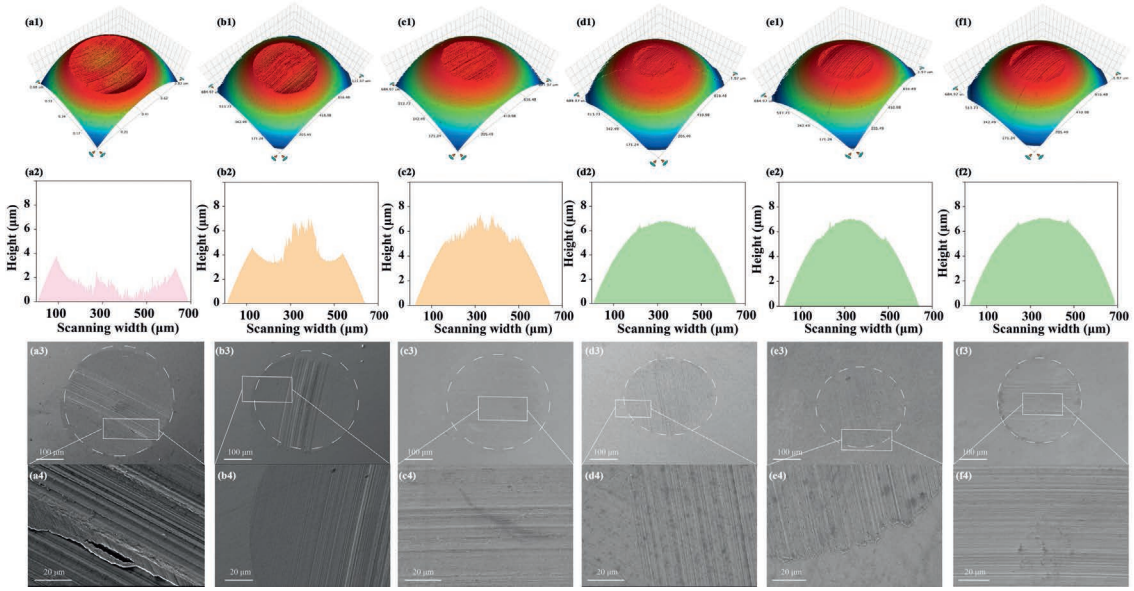


Fig. 3. The three dimensional (3D) morphology and corresponding cross-sectional profiles and scanning electron microscopy (SEM) of the worn surfaces with PAO (a_1, a_2, a_3, a_4), 7.5 wt% nano-gel (b_1, b_2, b_3, b_4),10 wt% nano-gel (c_1, c_2, c_3, c_4), 12.5 wt% nano-gel (d_1, d_2, d_3, d_4), 15 wt% nano-gel (e_1, e_2, e_3, e_4), 17.5 wt% nano-gel (f_1, f_2, f_3, f_4) at 1200 rpm, 294 N.

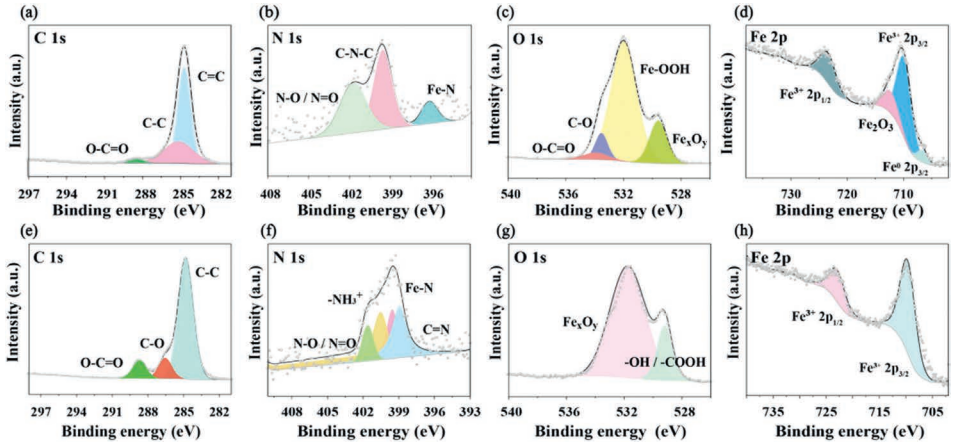


Fig. 4. XPS spectra of (a) C 1s, (b) N 1s, (c) O 1s, and (d) Fe 2p of the wear scars lubricated by PAO, (e) C 1s, (f) N 1s, (g) O 1s, and (h) Fe 2p of the of the wear scars lubricated by 12.5 wt% CPDs nano-gel at room temperature (294 N, 1200 rpm, 30 min).

To obtain a more intuitive observation the actual thickness of the tribofilm, randomly cutting the wear surfaces of the steel ball lubricated with CPDs nano-gel by focused ion beam (FIB) (Fig. 5). Figs. 5a and b showed that the thickness of the friction film is about 500–700 nm. A clear boundary was observed between Pt coating and Fe substrate, indicating the formation of a friction film on the metal surface, which was mainly composed of elements such as C, N, O by frictional degradation of PAO and CPDs in the gel system. From Fig. 5c, it can be observed that the C, N and O were uniformly distributed along the tribofilm layer without any element aggregation. The EDS in cross-sectional showed the main component of C in the friction film, which was the result of accumulation of a large amount of CPDs in the wear area. (Figs. 5c-h, Table S1 in Supporting information).

The anti-friction effect of the lubricant was directly affected by the thickness of the lubricating film. At the same time, the thickness of the lubricating film can also be made by the lubricating machine used to judge the lubricating agent. In this study, the steel surface has periodic wear and tear, so it is not suitable to measure the film thickness by optical interferometry. The four-ball friction and wear experiment belong to the point contact type. According to the Hamrock–Dowson [25] elliptical contact minimum film thickness (H_{min}) formula:

$$H_{min} = 3.63R_xU^{0.68}G^{0.49}W^{0.073}(1 - 0.61e^{-0.68k}) \quad (1)$$

where $U = \eta u/E'R_x$, $G = \alpha E'$, $W = w/(E'R_x{}^2)$. Specifically, η is the viscosity of the lubricant at room temperature, u ($\approx$0.399 m/s) is the relative sliding velocity, E' ($\approx 2.27 \times 10^{11}$ Pa) is the equivalent elastic modulus of steel ball and R_x ($\approx$3.175 mm) is the comprehensive radius of curvature of the ball. α ($\approx$15 GPa^{-1}) [26] refers to the viscosity-pressure coefficient of the lubricant, w is the experimental load, for the four-ball long grinding experiment, the experimental load is 294 N. The detailed calculation process for these parameters can be found in Supporting information. H_{min} is about 763 nm, which is close to what we measured in Fig. 5. Additionally, the lubrication state (λ) was classified using the following equation:

$$\lambda = \frac{H_{min}}{\sqrt{\sigma_1^2 + \sigma_2^2}} \quad (2)$$

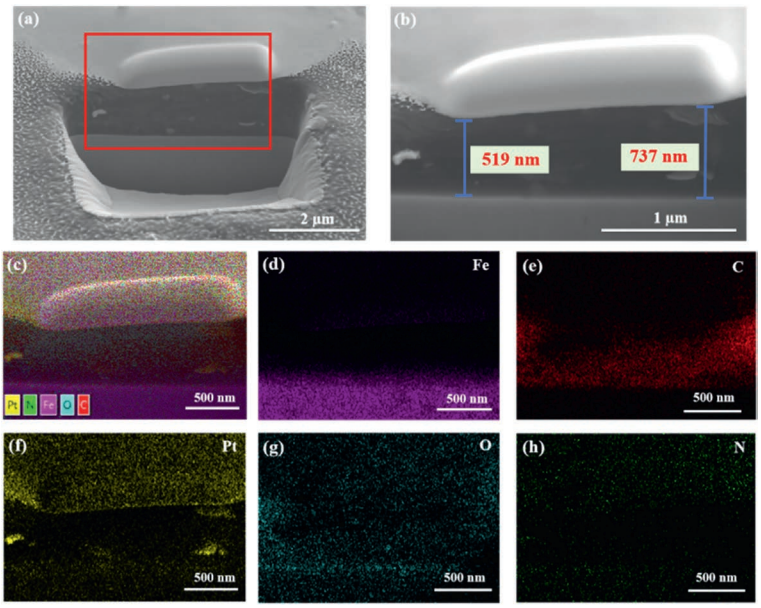


Fig. 5. Cross-sectional SEM image from focused ion beam (FIB) cutting worn surface lubricated with 12.5 wt% CPDs nano-gel (1200 rpm, 30 min, 294 N) in low (a) and high (b) magnification. Element distribution of tribofilm lubricated with 12.5 wt% CPDs. (c-h) Energy dispersive spectroscopy (EDS) mapping results for the tribofilm.

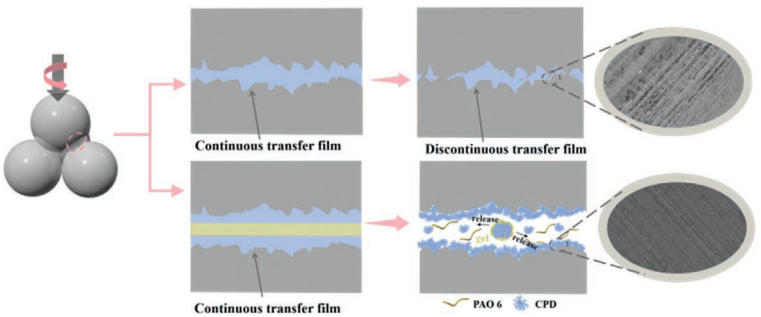


Fig. 6. Schematic diagram of lubrication mechanism.

where σ_1 (0.213) and σ_2 (0.189) are the average surface roughness of the wear trajectories of the top ball and the three bottom balls, respectively. In this work, it is calculated that the lubrication status of the PAO lubricant is in boundary lubrication ($\lambda = 0.35$), CPDs nano-gel lubricant is in mixed lubrication ($\lambda = 2.71$) (more details are available in the Table S2 in Supporting information).

Based on the above, the schematic diagram about the lubrication mechanism of CPDs nano-gel as lubricant shown in Fig. 6. Essentially, the friction between interfaces comes from relative sliding between surface micro-bulges. Therefore, minimizing direct contact between these micro-asperities is crucial for reducing interfacial friction. As for the friction pair between steel and steel lubricated by PAO, the friction-induced high temperatures accelerated the transformation of Fe_3O_4 to Fe_2O_3 [26,27]. As shown in Fig. 6, with the shear produced by friction, CPDs was released from the CPDs nano-gel because of shear-thinning properties, which was adsorbed on the surface of the Fe_2O_3, forming a friction film with excellent boundary lubrication [28]. Additionally, under high shear rates, the CPDs was released to enhances the viscosity of PAO, effectively enhancing the load-carrying capacity of the oil film. Based on the XPS of the wear marks (Fig. 4), it can be concluded that the main component of the lubricating film is iron oxide, which provides protection for the friction pair [29]. Based on the above characteristics, the CPDs nano-gel could be well applied in variable working conditions. However, the continuous increase of CPDs agent content does not always help lubrication. The shear resistance could be significantly improved because of the excessive CPDs, as shown in Fig. S6, obstructing the release of CPDs and PAO, ultimately degrading tribological performance and increasing friction and wear (Fig. 2). Thus, the best tribological performance can be achieved in the CPDs nano-gel system by adding 12.5 wt% CPDs.

In summary, a novel self-constraint CPDs nano-gel lubricant was fabricated by a facile yet efficient route. Unlike most gel based on the hydrogen bond, it enables gel to better disperse stress when experiencing external shear force and bearing pressure by dispersing stress to other molecular chains through dense entanglement, and avoid fracture and lubrication failure caused by local stress concentration. As an effective lubricant, the CPDs nano-gel played a key in friction reducing and anti-wear. The tribological test results revealed a notable decrease of 38.14 % in the COF and a 93.71 % decrease in the wear scar diameter of PAO when supplemented with 12.5 wt% CPDs. Further investigation into the wear surface and the calculation of the mathematical model, it was concluded that the unique lubrication effect of CPDs nano-gel might be due to the large supramolecular adsorption between the friction pairs to form a thicker oil film, thus reducing the wear loss. This study underscored the potential of utilizing carbonized polymer dots for self-assembly applications, and we anticipate that supramolecular carbonized polymer dots gels have great potential in lubrication and emission reduction by extending the mechanical life, ultimately contributing to the development of a sustainable society.

Supplementary material that may be helpful in the review process should be prepared and provided as a separate electronic file. That file can then be transformed into PDF format and submitted along with the manuscript and graphic files to the appropriate editorial office.

Declaration of competing interest

The authors declare that they have no known competing financial interests or personal relationships that could have appeared to influence the work reported in this paper.

CRediT authorship contribution statement

Pai Yu: Writing – original draft, Data curation. **Chenchen Wang:** Writing – review & editing, Project administration. **Hualin Lin:** Supervision, Funding acquisition. **Sheng Han:** Supervision, Funding acquisition.

Acknowledgments

This work was supported by the National Natural Science Foundation of China (Nos. 22075183, 22278269 and 21975161), Industrial Collaborative Innovation Project of Shanghai (Nos. 2021-cyxt1-kj37 and XTCX-KJ-2022-70), Talent scientific research start-up project (No. YJ2022–10) and Collaborative Innovation Fund (No. XTCX2024-02) from Shanghai Institute of Technology, Research and Innovation Project of Shanghai Municipal Education Commission (No. 2023ZKZD54), Shanghai "Science and Technology Innovation Action Plan" Morning Star Cultivation (Sailing Program, No. 22YF1447500) and “Chen Guang” project (No. 22CGA75) supported by Shanghai Municipal Education Commission and Shanghai Education Development Foundation, Talent scientific research start-up project (No. YJ2022–10) and Collaborative Innovation Fund (No. XTCX2024-02) from Shanghai Institute of Technology and Collaborative Innovation Center of Fragrance Flavour and Cosmetics.

Supplementary materials

Supplementary material associated with this article can be found, in the online version, at doi:10.1016/j.cclet.2025.111931.

References

[1] M. Cai, Q. Yu, F. Zhou, W. Liu, Friction 5 (2017) 361–382.
[2] L. Chen, C. Lin, D. Shi, et al., Nat. Commun. 14 (2023) 6323.
[3] K. Holmberg, P. Kivikytö-Reponen, P. Härkisaari, K. Valtonen, A. Erdemir, Tribol. Int. 115 (2017) 116–139.
[4] H. Liu, B. Yang, C. Wang, Y. Han, D. Liu, Friction 11 (2023) 839–864.
[5] K. Holmberg, A. Erdemir, Friction 5 (2017) 263–284.
[6] H. Liang, M. Liu, T. Yin, et al., Adv. Funct. Mater. 34 (2024) 2311600.
[7] S. Bond, R.L. Jackson, G. Mills, Friction 12 (2024) 796–811.
[8] S. Chen, Y. Fan, J. Song, B. Xue, Mater. Today Chem. 23 (2022) 100719.
[9] S.S. Babu, V.K. Praveen, A. Ajayaghosh, Chem. Rev. 114 (2014) 1973–2129.
[10] P.R.A. Chivers, D.K. Smith, Nat. Rev. Mater. 4 (2019) 463–478.
[11] R. Contreras-Montoya, L. Álvarez de Cienfuegos, J.A. Gavira, J.W. Steed, Chem. Soc. Rev. 53 (2024) 10604–10619.
[12] X. Jiang, C. Li, Q. Han, Mater. Today Chem. 31 (2022) 103700.
[13] J. Zou, Z. Lin, L. Zhan, et al., Carbohydr. Polym. 340 (2024) 122241.
[14] P. Yu, C. Wang, H. Lin, S. Han, Y. Mao, Carbon 233 (2025) 119829.
[15] J. Gu, S. Yuan, W. Shu, et al., Colloid Surface A 498 (2016) 218–230.
[16] R. Liang, H. Zhang, Y. Wang, et al., Chem. Eng. J. 442 (2022) 136204.
[17] I. Noda, Appl. Spectrosc. 47 (1993) 1329–1336.
[18] R. Wang, X.-Y. Liu, J. Xiong, J. Li, J. Phys. Chem. B 110 (2006) 7275–7280.
[19] F. Wang, X. Yu, M. Ge, S. Wu, Chem. Eng. J. 384 (2020) 123381.
[20] X. Chen, X. Wang, D. Fang, Fuller. Nanotub. Car. Nanostruct. 28 (2020) 1048–1058.
[21] F. Güneş, A. Aykaç, M. Erol, et al., J. Alloy. Compd. 895 (2022) 162688.
[22] G. Jin, Y. Cui, K. Yan, et al., Carbon 230 (2024) 119578.
[23] D. Wilson, M.A. Langell, Appl. Surf. Sci. 303 (2014) 6–13.
[24] H.J. Noh, H. Jang, Wear 400-401 (2018) 93–99.
[25] B.J. Hamrock, D. Dowson, J. Lubr. Technol. 98 (1976) 375–381.
[26] T. Wang, Y. Wang, X. Wang, et al., ACS Nano 18 (2024) 33468–33478.
[27] G. Jin, H. Li, Y. Cui, et al., J. Mater. Chem. A 13 (2025) 6737–6748.
[28] S. Xue, X. Zhang, Y. Wang, et al., Tribol. Int. 201 (2025) 110227.
[29] G. Jin, S. Xue, R. Zhang, et al., Small 20 (2024) 2311876.